Design, Synthesis, and in Vitro Biological Evaluation of Small Molecule Inhibitors of Estrogen Receptor α Coactivator Binding

Alice L. Rodriguez, Anobel Tamrazi, Margaret L. Collins, and John A. Katzenellenbogen*

Department of Chemistry, University of Illinois, 600 South Mathews Avenue, Urbana, Illinois 61801

Received August 19, 2003

Nuclear receptors (NRs) complexed with agonist ligands activate transcription by recruiting coactivator protein complexes. In principle, one should be able to inhibit the transcriptional activity of the NRs by blocking this transcriptionally critical receptor−coactivator interaction directly, using an appropriately designed coactivator binding inhibitor (CBI). To guide our design of various classes of CBIs, we have used the crystal structure of an agonist-bound estrogen receptor (ER) ligand binding domain (LBD) complexed with a coactivator peptide containing the LXXLL signature motif bound to a hydrophobic groove on the surface of the LBD. One set of CBIs, based on an outside-in design approach, has various heterocyclic cores (triazenes, pyrimidines, trithianes, cyclohexanes) that mimic the tether sites of the three leucines on the peptide helix, onto which are appended leucine residue-like substituents. The other set, based on an inside-out approach, has a naphthalene core that mimics the two most deeply buried leucines, with substituents extending outward to mimic other features of the coactivator helical peptide. A fluorescence anisotropy-based coactivator competition assay was developed to measure the specific binding of these CBIs to the groove site on the ER−agonist complex with which coactivators interact; control ligand-binding assays assured that their interaction was not with the ligand binding pocket. The most effective CBIs were those from the pyrimidine family, the best binding with K_i values of ca. 30 μM. The trithiane- and cyclohexane-based CBIs appear to be poor structural mimics, because of equatorial vs axial conformational constraints, and the triazene-based CBIs are also conformationally constrained by amine-substituent-to-ring resonance overlap, which is not the case with the higher affinity alkyl-substituted pyrimidines. The pyrimidine-based CBIs appear to be the first small molecule inhibitors of NR coactivator binding.

Introduction

Nuclear receptors (NRs) are ligand-modulated transcription factors that mediate the action of steroid hormones and various other bioactive ligands. The members of the NR gene superfamily have distinct domain structures, with a highly conserved DNA-binding domain (domain C) and a moderately conserved ligand-binding domain (LBD, domain E) being separated by a nonconserved hinge domain (domain D) and flanked by an N-terminal modulatory domain (A/B domain) and a C-terminal region (F domain). Many of the actions of NRs are initiated by hormone binding to the LBD, a process that stabilizes the conformation of this domain. When an agonist ligand binds to an NR LBD, this conformational stabilization rigidifies surface features that function as docking sites for the nuclear receptor interaction regions of different coregulatory protein complexes.[1,2]

Of the coregulator complexes implicated in NR action, the most fully investigated is the chromatin-modifying complex, in which a protein from the p160 class of coactivators, also called steroid receptor coactivators (SRCs), binds to the NR and functions as a platform protein for the docking of other proteins (CBP/p300, pCAF, CARM, etc.) that have enzymatic activity for derivatizing histones (acetylation, phosphorylation, methylation).[1,2] X-ray crystal structures have been obtained of several NR−agonist complexes with peptides or protein fragments of p160 coactivators encompassing one or more of the nuclear receptor interaction boxes (NR boxes) that contain the signature LXXLL sequence motif.[3−11] These structures show that the coactivator interacts with the NR LBD through a two-turn amphipathic α-helical motif that places the first and third leucine residues in a deep, but short, hydrophobic groove that is made up of several residues from helices 3, 4, 5, and 12 of the LBD. In addition, the intrinsic dipole moment of the coactivator helix is aligned with polar residues, a glutamate residue at its N-terminus, and a lysine residue at its C-terminus in the case of the estrogen receptor (ER), which together form a "charge clamp" for the coactivator helix within the ER LBD.

The general strategy used thus far to block the action of NR hormones has been to develop antagonists or antihormones. Such compounds compete with agonist ligands for binding to the ligand binding pocket, and upon binding they induce different conformations in the LBD.[3,4,9,12−14] These antagonist conformations either preclude the binding of the coactivators, by repositioning the C-terminal LBD helix 12 so that it occupies the coactivator binding groove itself, or they facilitate the binding of corepressor proteins by disposing helix-12 away from the LBD itself.

* To whom correspondence should be addressed. Phone: 217 333 6310. Fax: 217 333 7325. E-mail: jkatzene@uiuc.edu.

10.1021/jm030404c CCC: $27.50
Published on Web 12/30/2003

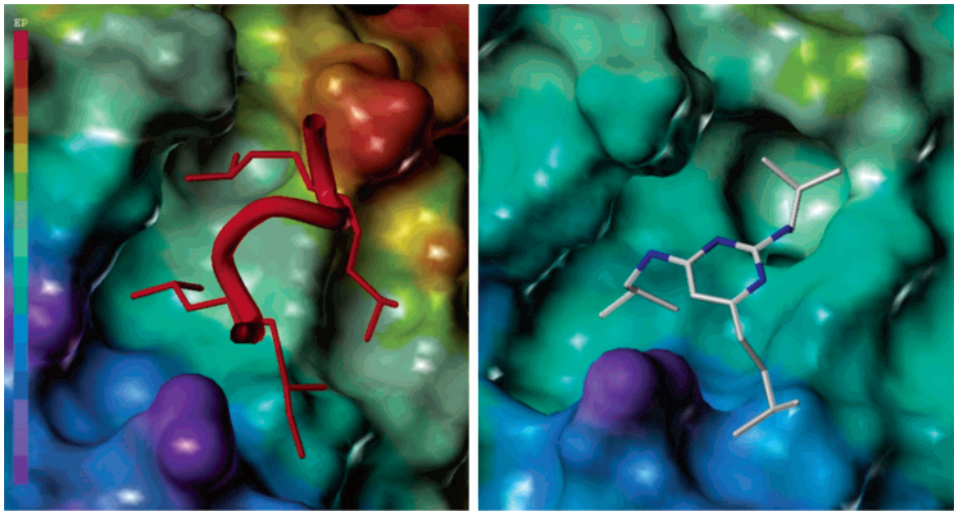

Figure 1. Electrostatic surface rendering of (A) the crystal structure of GRIP1 peptide bound to ERα and (B) pyrimidine CBI **12a** docked into ERα. The receptor is shown as a continuous surface where red coloring indicates positive charge and blue coloring indicates negative charge. **12a** is colored by atom type, whereas the coactivator peptide is depicted as a red tube.

Curiously, the effectiveness of NR antagonists can be compromised by cellular adaptations that seem to enable coactivators to bind to NR−antihormone complexes.[15] This appears to be the case with the development of tamoxifen resistance in the treatment of breast cancer: In tamoxifen-resistant breast tumor cells, the ER complex with *trans*-4-hydroxytamoxifen, the bioactive metabolite of tamoxifen, seems able to interact with coactivators, thereby—remarkably—reversing its role and activating rather than repressing transcription.[16,17]

An alternative approach to inhibiting the gene-regulating effects of NRs might be to develop compounds capable of blocking NR−coactivator interaction itself. A proof-of-principle demonstration of the effectiveness of this approach is the observation that peptides having the LXXLL sequence are able to block gene transcription induced by estrogen agonists working through the estrogen receptor (ER).[18,19] Thus, small molecule analogues that could perform the same function as these peptides—acting as coactivator binding inhibitors (CBIs) that block the ER−SRC interaction—might have a net antagonist effect that was independent of ER ligand binding. This approach to antagonizing the action of the ER might not be compromised by cellular adaptations, such as increased expression of certain coactivator proteins[15] or covalent modifications of the coactivators or the ER itself,[16,17] that are able to surmount the antagonist effect of ligand-based antiestrogens, such as tamoxifen.

In this report, we describe de novo, structure-based design approaches we have developed to prepare two types of coactivator binding inhibitors, and we present an in vitro assay method through which we can demonstrate that some of these compounds are able to block the interaction of ER with NR box peptides. Thus, we provide the first proof-of-principle that small molecules can function as effective inhibitors of the binding of coactivator proteins to the estrogen receptor.

Results

Structure-Based Design of Coactivator Binding Inhibitors. We have based our design of CBIs on a recent crystal structure of the ERα LBD complexed with diethylstilbestrol and a 13 amino acid peptide derived from the p160 class coactivator, GRIP1 (SRC-2),[1,2] containing a single NR box (Figure 1A). The interaction surface in the ER consists of 16 amino acid residues from helices 3, 4, 5, and 12: L354, V355, I358, A361, K362 (helix 3); L372 (helix 3,4 turn); F367, V368 (helix 4); Q375, V376, L379, E380 (helix 5); and D538, L539, E542, M543 (helix 12). Three zones of interaction are evident: L690 and L694 of the coactivator peptide are entirely engulfed by the ER, forming a deep, strong hydrophobic *groove* interaction; I689 and L693 of the coactivator peptide interact with the receptor on one-half of their surface, forming a weaker but apparently significant *surface* hydrophobic interaction; E542 and K362 of the ER form the *charge clamp* properly aligned for interaction with the inherent dipole of the α-helix and finally various amide functionalities on the helix backbone, locking and holding the hydrophobic side chains into position.

Class I Design. The first approach we took to designing small molecule inhibitors of coactivator binding was termed the "outside-in" approach. A head-on view of the coactivator peptide shows that the positions of the three leucine residues in the LXXLL signature sequence motif, as registered by their C_α atoms, fall roughly into the shape of an equilateral triangle, as shown in Figure 2. Thus, in this approach, a central core having dimensions corresponding to this C_α triangle was first chosen, and then hydrophobic substituents were attached in a manner that mimics—in a topologically faithful fashion—the positions of the three leucine residues of the coactivator peptide. Molecular modeling was used to refine the design of these class I inhibitors. These CBIs are said to follow an *outside-in* design, because they begin with a mimic for the helix backbone, which is *outside* of the hydrophobic groove, and then proceed *inward* by adding residue elements.

Four scaffolds were chosen as candidate cores for the class I CBIs: triazene, pyrimidine, trithiane, and cyclohexane. Hydrophobic substituents were then placed in alternate positions around the rings to mimic the leucine residues, and in some cases, polar functionalities were added to interact with the charge clamp residues

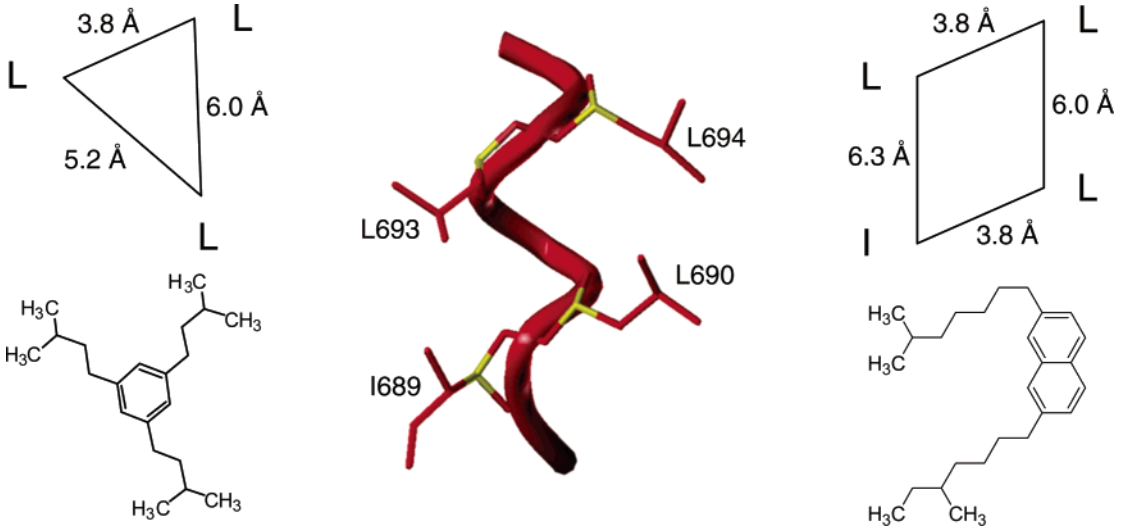

Figure 2. Class I and class II approaches to rational design of ERα coactivator-binding inhibitors (CBIs). The central figure depicts the GRIP1 coactivator peptide from which we based our design with NR box residues indicated by single letter amino acid notation. The Cα carbons are colored yellow. Class I design is shown to the left of the helix while class II design in shown to the right. The atomic distances between the Cα carbons of the NR box residues are indicated in each design and are mimicked by the residue elements in the CBIs.

in the ER LBD. Molecules were built using a molecular modeling platform (SYBYL), minimized, and then overlaid onto the coactivator peptide. Adjustments were made to the design, and the molecule was then reminimized and docked into the coactivator binding groove. A set of compounds was then chosen for synthesis based on a combination of molecular modeling results and relative ease of synthesis. Further structural issues related to specific scaffolds in the outside-in design are discussed in the Synthesis section.

Class II Design. We termed our second approach to CBIs the "inside-out" design. From the face of the α-helix, the four hydrophobic residues of the NR box approximate the shape of a parallelogram, as shown in Figure 2. Accordingly, we envisioned using a hydrophobic small molecule to mimic both of the most deeply buried *groove* residues, L690 and L694, which are considered most crucial for stabilizing the ER−coactivator interface. We hypothesized that a hydrophobic unit of appropriate dimensions could be used to fill the groove portion of the coactivator binding pocket, without specifically mimicking the shape of the individual leucine residues. From this hydrophobic small molecule mimic of the two *inside* leucines, flexible linkers then extend *outward*, hence the term *inside-out* design. These linkers would incorporate other relevant functionalities, including the two remaining hydrophobic residues, I689 and L693, and in some cases the polar charge-clamp functionalities. Following the modeling protocol discussed above, compounds derived from substituted naphthalenes were chosen for synthesis.

Synthesis. Triazenes. Triaminotriazenes were synthesized in a single step from commercially available cyanuric chloride (Scheme 1). Triazene **1a** was synthesized by reacting cyanuric chloride with isobutylamine to produce a compound having substituents that directly mimic the three branched leucine amino acids. Triazenes **1b**−**e** were synthesized by reacting cyanuric chloride with a variety of alkyl- and arylamines containing simple straight-chain and cyclic alkyl and aryl substituents.

Scheme 1. Synthesis of Triazene-Core CBIs

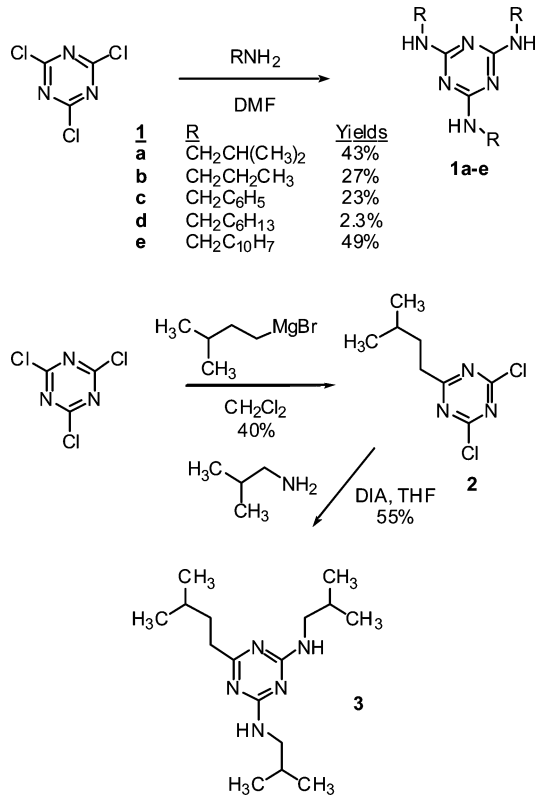

We expanded our study of the triazene class of compounds to include ones containing substituents linked directly through a carbon atom rather than nitrogen. By obviating the resonance interaction of the substituent nitrogen lone pair with the triazene ring, this carbon-for-nitrogen substitution increases the torsional flexibility of the substituents and effectively eliminates the steric energy penalty encountered when the isobutyl substituents of these triazene mimics are overlapped with three leucines in the coactivator peptide. In fact, using MacroModel, we estimate that the torsional barrier for rotation of a *nitrogen* substitutent

Scheme 2. Synthesis of Other Triazene-Core CBIs

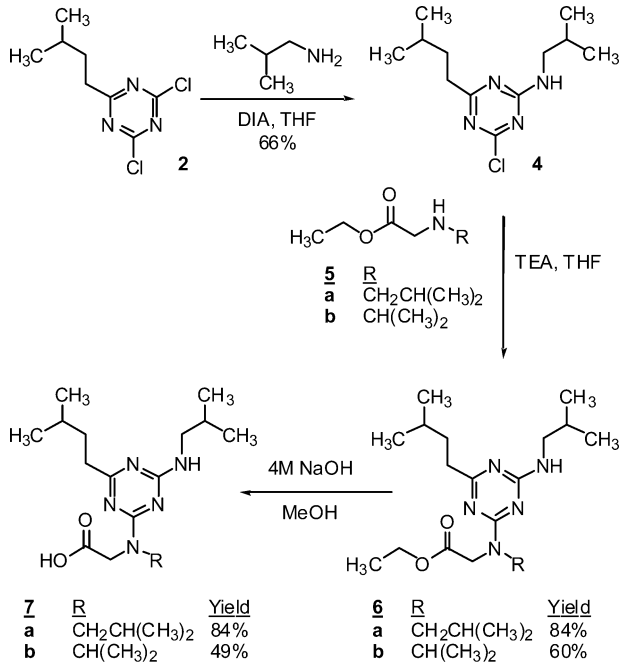

5	R
a	$CH_2CH(CH_3)_2$
b	$CH(CH_3)_2$

7	R	Yield
a	$CH_2CH(CH_3)_2$	84%
b	$CH(CH_3)_2$	49%

6	R	Yield
a	$CH_2CH(CH_3)_2$	84%
b	$CH(CH_3)_2$	60%

on a triazene to be ca. 9 kcal/mol, whereas rotation of a *carbon* substituent on a triazene or pyrimidine is less than 2 kcal/mol. The synthesis of a monoalkylated triazene began with the addition of 3-methylbutylmagnesium bromide to cyanuric chloride. This reaction was run at low temperatures to minimize over addition of the Grignard reagent. Subsequent addition of an excess of isobutylamine afforded the differentially trisubstituted triazene **3**.

To incorporate an acid functionality for interaction with K362 involved in the charge clamp, intermediate **2** was reacted with a single equivalent of isobutylamine to give disubstituted triazene **4** (Scheme 2). Amines **5a,b** were synthesized according to literature procedures (as described in the Supporting Information) and were reacted with the disubstituted triazenes **4** to give fully substituted products **6a,b**. Hydrolysis of the esters provided the desired triazenes **7a,b**. The predicted torsional rigidity of the C−N bonds of the amine substituents became apparent with the addition of the final amines. Variable-temperature ^{1}H NMR spectroscopy demonstrated the presence of two rotameric species in each case (data not shown).

Pyrimidines. As discussed in the triazene section, pyrimidine compounds were examined because they have greater torsional flexibility than the triazene compounds. A series of pyrimidine core CBIs was synthesized by reacting β-keto esters **8a**−**c** with thiourea to afford thiouracil derivatives **9a**−**c** (Scheme 3). The β-keto esters were either commercially available (**8b**) or were made conveniently from the corresponding aldehyde or ketone. Reaction of the aldehyde with ethyl diazoacetate and $SnCl_2$ provided the desired β-keto esters in the case of **8c**. Reaction of the methyl ketone with sodium hydride and diethyl carbonate provided the β-keto ester **8a**.

The thioketone moiety of the thiouracils **9a**−**c** was converted to a ketone by reaction with chloroacetic acid. This transformation is thought to proceed through a spirolactone intermediate, which upon hydrolysis provides uracil derivatives **10a**−**c** and mercaptoacetic acid as a byproduct. Phosphorus oxychloride transformed uracils **10a**−**c** to dichloropyrimidines **11a**−**c**. Reaction of the dichloropyrimidines **11a**−**c** with the appropriate amine afforded the desired series of pyrimidines **12a**−**c**. Both monoaminated products were obtained as byproducts in most cases, contributing to decreased yields in the final step.

Scheme 3. Synthesis of Pyrimidine-Core CBIs

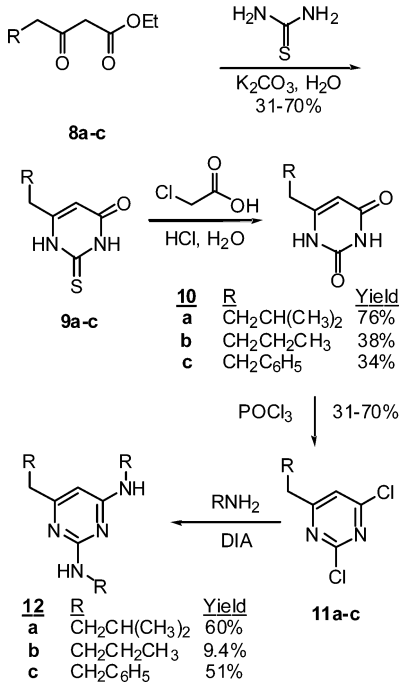

10	R	Yield
a	$CH_2CH(CH_3)_2$	76%
b	$CH_2CH_2CH_3$	38%
c	$CH_2C_6H_5$	34%

12	R	Yield
a	$CH_2CH(CH_3)_2$	60%
b	$CH_2CH_2CH_3$	9.4%
c	$CH_2C_6H_5$	51%

Scheme 4. Synthesis of Trithiane- and Cyclohexane-Core CBIs

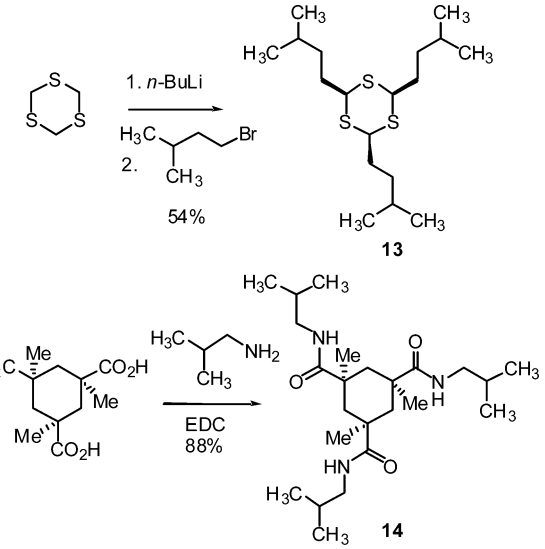

Trithiane. The CBI containing a trithiane core was synthesized from commercially available 1,3,5-trithiane (Scheme 4). The starting material was reacted with *n*-BuLi, followed by 1-bromo-3-methylbutane in three successive additions, to yield the trisubstituted trithiane **13**. According to the literature, a single conformational isomer with all three alkyl substituents in the equatorial positions is obtained by controlling the temperature of addition. By performing the lithiation step at −45 °C and the substitution at −20 °C, a single isomer was

Scheme 5. Synthesis of Naphthalene-Core CBIs

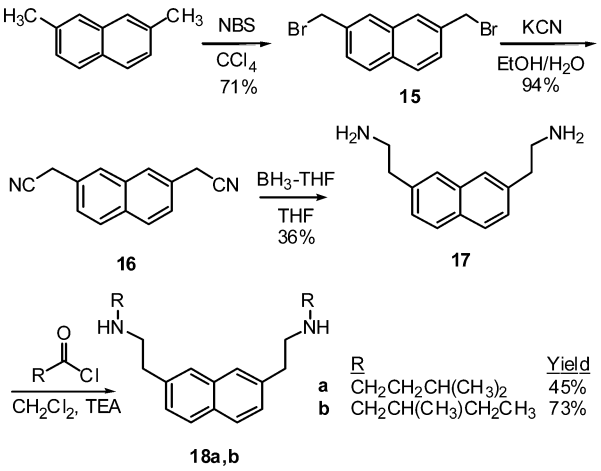

obtained. On the basis of the symmetry evident in the ^{1}H NMR spectrum, it is presumed to be the all-equatorial isomer (data not shown). The conversion of this triequatorial trialkyltrithiane to the all-axial conformation, as is needed to achieve good three-dimensional overlap between the three substituents and the three leucine residues in the NR box helix, undoubtedly involves a increase in steric energy. We have estimated this increase to be ca. 5 kcal/mol, on the basis of molecular mechanics calculations on both conformers (using the MMFF94 force field within SYBYL).

Cyclohexane. CBI **14** containing a cyclohexane core was prepared in a single step from commercially available Kemp's triacid (KTA), as seen in Scheme 4. KTA is a useful cyclohexane core mimic because its conformational preference is just the opposite that of the 1,3,5-trithianes. KTA is locked into a chair conformation with the acid groups in the axial positions, as a result of intramolecular hydrogen bonding between the acid groups. KTA was coupled to isobutylamine under standard coupling conditions, using EDC as a coupling reagent.

Naphthalenes. Bromination of the commercially available 2,7-dimethylnaphthlene afforded **15**, which was reacted with potassium cyanide to give bisnitrile **16** (Scheme 5). Reduction of the nitrile functionality to the primary amine was accomplished using borane−THF, providing the bis(aminoethyl)-substituted intermediate **17**. Reaction of both of these amines with acid chlorides yielded the naphthalene-based CBIs **18a,b**.

The Binding of Coactivator Binding Inhibitors to the Estrogen Receptor. Fluorescence Anistropy Assay. To evaluate the potential of our CBIs to bind to the ER LBD in a manner that competes with the binding of coactivators, we developed a simple competitive binding assay, using a fluorophore-labeled coactivator peptide. Anisotropy measurements are ideally suited for studying the association of fluorescent peptides to proteins,[20,21] because the low anisotropy of the rapidly tumbling free peptide (MW ca. 1500) increases when its mobility becomes restricted as a result of its binding to a large protein such as the ER LBD (MW ca. 60 000 for the LBD dimer). As the peptide−fluorophore tracer, we utilized an eight amino acid peptide containing a single NR box with the sequence NH_2−IL-RKLLQE−CO_2H to mimic the coactivator protein. It

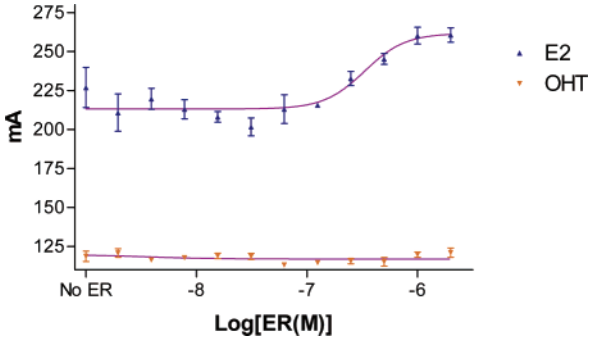

Figure 3. Recruitment of TMR-labeled NR box peptide to the ER as followed by fluorescence anisotropy. Estradiol-bound ER (E2) recruits the peptide as demonstrated by an increase in anisotropy, whereas hydroxytamoxifen-bound ER (OHT) does not recruit the peptide.

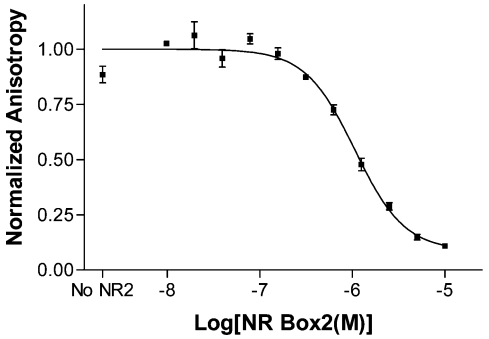

Figure 4. Displacement of TMR-labeled NR box peptide by unlabeled NR box 2, as shown by fluorescence anisotropy.

was labeled at its N-terminus with tetramethylrhodamine (TMR), a fluorophore chosen for its short lifetime and low environmental sensitivity.[20]

An ER titration was performed to validate the binding of the labeled peptide to the ER, and the apparent K_d of the peptide was found to be 190 nM (Figure 3). Interestingly, the addition of the fluorophore markedly increased the affinity of the peptide for the ER when compared to the unlabeled octapeptide, which was ca. 5 μM. TMR is a hydrophobic molecule, which could make favorable contacts with hydrophobic regions around the coactivator binding groove. A similar titration was performed by replacing the agonist ligand estradiol with the antagonist ligand *trans*-4-hydroxytamoxifen (OHT) (Figure 3). In this case, no increase in anisotropy was observed, because the conformational change in the ER induced by antagonist binding renders the receptor unable to recruit coactivator proteins or peptides.

A competition was performed to validate that the labeled peptide is binding in the coactivator binding groove (Figure 4). A 15 amino acid peptide containing a single NR box, specifically the second NR box in SRC-1 (SRC-1-NR box 2, CLTERHKILHRLLQE), is known to bind to the ER in the coactivator groove with a K_d of approximately 1 μM.[22,23] In this experiment, the concentration of the labeled peptide was maintained at 20 nM, while an increasing amount of SRC-1-NR box 2 was added, reaching a maximum of 100 μM. The anisotropy significantly decreased (by 130 mA units, which is ca. 33% of the theoretically possible range),[20] indicating displacement of the labeled peptide by SRC-1-NR box 2. In this experiment, the K_i value for the SRC-1-NR box 2 peptide was estimated to be 700 nM, similar to previously reported values for this NR box.[22,23]

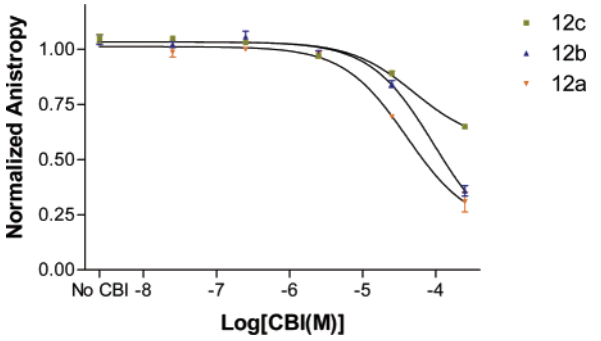

Figure 5. Displacement of TMR-labeled peptide by pyrimidine CBIs.

Table 1. Summary of Binding Affinity Data for Triazene, Pyrimidine, Trithiane, Cyclohexane and Naphthalene CBIs

CBI	K_i (μM)	CBI	K_i (μM)	CBI	K_i (μM)
1a	590	**3**	650	**12c**	49
1b	290	**7a**	790	**13**	>1000
1c	240	**7b**	410	**14**	>1000
1d	290	**12a**	29	**18a**	>1000
1e	290	**12b**	32	**18b**	>1000

Biological Evaluation. The Class I compounds containing a triazene core showed weak inhibition of coactivator peptide binding (Table 1). The most potent triazene was **7b**, which showed a minimal decrease in anisotropy. Addition of polar functionalities improved the binding slightly in the case of **7b**, but did not improve binding in any other case. In fact, for the symmetric triaminotriazenes there appears to be virtually no improvement in binding as the hydrophobic functionality of the substituents is varied. The weak inhibitory activity of this class of compounds might be due to the inherent rigidity of the triaminotriazene core, as discussed previously. The partial double bond character of the C−N bond directly attached to the triazene core may prevent the compounds from adopting a conformation optimal for binding to the ER.

By contrast, the class I compounds containing a pyrimidine core showed the most promise as CBIs (Figure 5). Compound **12a**, which contains branched alkyl substituents that directly mimic L690, L693, and L694, displaces the TMR-labeled coactivator peptide with a K_i of 29 μM. By directly comparing the results of pyrimidine **12a** with those of triazene **1a**, the conclusion can be drawn that the increased affinity of **12a** results from the increased torsional flexibility of its two additional methylene units.

After we obtained the initial results with the lead pyrimidine **12a**, we prepared additional pyrimidines that contained varying hydrophobic subtituents, including a straight-chain alkyl group and an ethylphenyl substituent, to probe the capacity of the coativator binding groove to accommodate different hydrophobic units. The binding behavior of these additional compounds in the pyrimidine series varied. Pyrimidine **12c** with terminal phenyl substituents inhibited recruitment of coactivator peptide with a K_i of 49 μM, being somewhat less effective than the direct leucine mimic **12a**. Pyrimidine **12b** with straight-chain alkyl substituents inhibited recruitment of the labeled peptide with a K_i of 32 μM, very similar to the lead pyrimidine **12a**. These results demonstrate that the coactivator binding pocket can tolerate hydrophobic substituent functionalities that differ from the direct branched leucine mimics.

CBIs **13** and **14** containing trithiane and cyclohexane cores, respectively, showed virtually no affinity for the coactivator binding groove (Table 1). When compound **14** was designed, it was hoped that the prepositioned axial stereochemistry of the side chains would force the leucine mimics into the same direction and into the coactivator groove, thereby producing an effective CBI. Molecular modeling shows the Kemp's triacid core **14** to be somewhat smaller than the coactivator peptide when the two are overlaid. Thus, it is possible that the hydrophobic side chains are too close together and thus unable to span the groove in a productive binding mode.

Class II CBIs containing a naphthalene core displayed weak binding to the receptor, as shown by fluorescence anisotropy (Table 1). Compounds **18a,b**, which contain functionalities mimicking all four hydrophobic portions of the coativator, showed weak binding at high concentrations. It did not make a difference whether the flexible side chains contained leucine or isoleucine mimics. These initial studies lead us to believe that the naphthalene class of compounds does not show promise as CBIs. It may be that the naphthalene unit itself is too planar or too thin to sufficiently fill the deep hydrophobic groove, or that the class II "inside-out" design concept is not practical when applied.

Lack of CBI Binding in the Ligand Binding Pocket. In assaying compounds for inhibition of coactivator binding, it is essential to establish that this inhibition arises from a *direct* competition between the CBI and the coactivator peptide at the coactivator binding groove, rather than by an *indirect* competition at the ligand binding pocket of the LBD. The latter, indirect process would involve small molecule binding to the ligand binding pocket in the same manner as an antagonist, inducing a conformation of helix 12 that occludes the coactivator binding groove and thus indirectly precludes coactivator binding. To ensure that the inhibition of coactivator binding we observe is not due to the indirect binding mechanism, we have measured the affinity of the CBIs for the ligand binding pocket of ERα, using a competitive radiometric binding assay with [^{3}H]estradiol (data not shown). Our most effective CBI, pyrimidine **12a**, has an affinity of 0.01% that of estradiol (estradiol is set at 100%), and the rest of our CBIs have an affinity equal to or lower than **12a**. Because the concentration of estradiol used in the CBI assay is 10 μM, we can estimate that the IC_{50} for competition by an indirect mechanism would be 100 mM. Because we measure an IC_{50} of 32 μM for this compound, we can conclude that it is competing for coactivator binding by a direct mechanism.

Molecular Modeling. We have also used molecular modeling to investigate the possible binding orientation of lead pyrimidine **12a** in ERα. Using the FlexiDock routine in the molecular modeling platform SYBYL, we docked pyrimidine **12a** into the receptor. Initially, the pyrimidine was overlayed onto the coactivator peptide by aligning each CH group in the branched side chains with those in the side chains of L690, L693, and L694. The result of this docking-minimization study is shown in Figure 1B, adjacent to a rendering of the ERα-

coactivator peptide crystal structure for comparison. The receptor is shown as a continuous electrostatic surface, where red coloring indicates positive charge and blue coloring indicates negative charge. The CBI **12a** (Figure 1B) is colored by atom type, with hydrogens removed for clarity, whereas the coactivator peptide (Figure 1A) is depicted as a red tube, with extraneous side chains removed for clarity.

This final minimized model shows two alkyl substitutuents of CBI **12a** projecting downward into the deep hydrophobic groove of the receptor, filling the area normally occupied by L690 and L694. The third alkyl substituent sits comfortably on the hydrophobic shelf occupied by I689 in the ERα crystal structure. The interaction between pyrimidine **12a** and the receptor appears to be entirely hydrophobic in nature, as indicated by the lack of hydrogen bonding or electrostatic interactions in this model. In fact, one should recall that attempts to engage the charge clamp interactions in the CBIs of triazene design did not improve binding affinity. Significantly, in the model of pyrimidine **12a** binding to ER, the charge clamp residue K362 is repositioned: In the crystal structure of the ER-DES/GRIP1 NR-2 box peptide, the lysine residue extends outward from the receptor and is involved in a polar interaction with the coactivator peptide; however, because pyrimidine **12a** contains no hydrogen bond or polar partners for K362, this residue no longer projects outward from the receptor. Instead, it repositions itself in such a manner that it hydrogen bonds with Q375 and pinches off one end of the coactivator binding groove. This creates a smaller hydrophobic pocket that better matches the size of the smaller pyrimidine when compared to the coactivator peptide.

It is worth noting that, through our various docking studies, we have found the coactivator binding groove to be a fairly flexible surface. In fact, it can expand or contract to accommodate molecules both larger and smaller than the coactivator peptide from which we based our design. The charge clamp residues, which in part determine the "length" of the hydrophobic groove, are also able to bend and stretch to reach an optimal position when docking small molecules, as we found in our docking of pyrimidine **12a**. The implications of this apparent flexibility of the coactivator binding groove in terms of the development of small molecule CBIs by design will only become clear as more and more compounds are explored.

Discussion

The development of compounds that can block the interaction of agonist−liganded nuclear receptors with coactivator proteins could provide unique pharmacological tools for interrupting the signal transduction cascade of these transcription regulators. In this paper, we have described an approach to developing small molecule coactivator binding inhibitors (CBI) by a de novo, structure-inspired approach, and we have evaluated a set of candidate CBIs for their activity in blocking the binding of a model nuclear receptor interaction box (NR box) peptide. Thus far, of the two design approaches we have taken (class I, outside-in; class II, inside out) and the various types of CBIs we have investigated, only compounds from the class I series were found to be effective in blocking the interaction of a coactivator NR box peptide with the ER, and the best of these were in the pyrimidine series. The trithiane-based and Kemp triacid-based CBIs are probably poor structural mimics of the bound coactivator peptide, the former being too wide (triequatorial) and the latter too narrow (triaxial). The class I CBIs in the triazene series are less effective than the pyrimidines, probably because they are also more conformationally constrained from reaching a geometry that effectively mimics the bound coactivator peptide, the result of amine-substituent-to-ring resonance overlap. Although the 1,3,5-substituent display of the triazenes and the pyrimidines are essentially identical, we made a conscious decision to minimize this torsional constraint by investigating the alkyl-substituted triazenes and pyrimidines.

The most extensive work on the interruption of nuclear receptor coactivator interaction has been done by McDonnell and co-workers, using short peptides generated by phage display. Most of the peptides identified by screening contained a canonical LXXLL NR box, and some were able to discriminate between ERα and ERβ, and among ERs complexed with ligands of different structure, including some antagonists.[24−27] These findings highlight the fact that the topographical features of the coactivator binding groove reflect not just nuclear receptor subtype but also the detailed structure of the ligand bound to the receptor, that sequences flanking the NR box may also play a role in nuclear receptor subtype selectivity,[28] and that interaction sites persist in the ER complexes with antagonists, despite the apparent occlusion of the coactivator groove by the antagonist-induced displacement of helix 12 shown by X-ray structures.[3,4,12,13] In addition, some of these peptides were found to disrupt ER-mediated transcription induced by estrogen agonists in target cells; certain peptides even blocked the partial agonism shown in some cells by the antiestrogen tamoxifen, suggesting that a blockade of ER signaling at the level of NR−coactivator interaction might prove effective in overcoming tamoxifen resistance that often develops in the treatment of breast cancer.[18,19]

In the area of nonnatural peptide-based CBIs for nuclear receptors, Guy and co-workers demonstrated that the binding affinity of an NR box peptide could be increased by up to 15-fold by introducing chemical modifications in the residues (e.g., macrolactamization) that stabilize the α-helical conformation.[29] In libraries of similarly constrained peptides containing nonnatural α-amino acids in place of the leucines in the LXXLL motif, this group found that members differing at only one site of substitution showed a 600-fold preference for binding to ERα vs ERβ or TRβ.[30] This large degree of selectivity among members of the nuclear receptor family provides encouragement that similar selectivity might eventually be achieved with small, nonpeptide-based CBIs. More recently, Leduc and co-workers[31] described other amide and disulfide constrained LXXLL peptides as CBIs. The latter analogues, in particular, bound to the ERα with high affinity and good selectivity; although these analogues were found not to be helical when free in solution, they were shown by X-ray analysis to adopt a helical structure when bound to the ER.

Inhibition of protein−protein interactions with small molecules is a relatively young field with a number of unique challenges.[32,33] Often, protein−protein binding occurs over a relatively large surface area, which makes it difficult to focus on essential, high-affinity interactions that might be blocked with low molecular weight organic molecules. Sometimes, the binding surface between two proteins is relatively "smooth", lacking grooves or pockets that make good sites for small molecule binding. Despite these challenges, there are examples of small molecules acting as potent and specific inhibitors of various protein−protein interactions, including the helix−groove interactions of the type we have been investigating. Hamilton and co-workers developed a terphenyl scaffold to mimic extended regions of an α-helix, using these helix analogues to inhibit gp41 assembly and viral fusion and to block the binding of Bcl2 to Bcl-x_L, which regulates apoptosis.[34−36] These are longer helix−groove interactions that involve three turns of the α-helix (vs two turns for the NR coactivator interactions), and the substituents on the terphenyl core nicely mimic the *i*, *i* + 4, *i* + 7 sites of a three-turn α-helix, as do substituents on a related oligoamide foldamer.[37] Using computer-based screening strategy, Huang and co-workers discovered small molecules that inhibited Bcl-2 function by competing for its binding to Bcl-x_L.[38−41] More recently, Asada and co-workers screened a library of tryptophan derivatives to find an inhibitor of the interaction of a helical element of the nuclear protein ESX with the Sur-2/DRIP130 transcription factor.[42] The best inhibitor, a derivative of pindolol, termed adamanolol, had a K_i of 8 μM, which is similar to that of our best pyrimidine **12a**.

Our discovery that certain small molecules, particularly the 2,4,6-trialkyl-substituted pyrimidines, are able to inhibit coactivator binding to the estrogen receptor, provides a proof-of-principle that effective small molecule CBIs can be developed. The highest affinity CBI that we have identified so far, pyrimidine **12a**, however, has a K_i of 29 μM, which is insufficient for it to be studied effectively in cell culture or in vivo models of estrogen action (Katzenellenbogen et al., unpublished). Nevertheless, these pyrimidine CBIs appear to be the first small molecule inhibitors of nuclear receptor coactivator binding that have been reported. We are pursuing further refinements in the design of CBI to improve their binding affinity.

Experimental Section

General Methods. All reagents and solvents were obtained from Aldrich or Fisher. Tetrahydrofuran, diethyl ether, and dichloromethane were dried by the solvent delivery system (SDS) (neutral alumina columns) designed by Meyer.[43] Triethylamine, diisopropylamine, and diethyldiisopropylamine were distilled from and stored over potassium hydroxide pellets. Butyllithium was titrated using *N*-pivaloyl-*o*-toluidine, according to a literature method.[44] All reactions were performed under a dry (Drierite) nitrogen atmosphere unless otherwise stated.

Reaction progress was monitored using analytical thin-layer chromatography (TLC) on 0.25 mm Merck F-254 silica gel glass plates. Visualization was achieved by either UV light (254 nm) or potassium permanganate indicator. Flash chromatography was performed with Woelm silica gel (0.040−0.063 mm) packing. ^{1}H and ^{13}C spectra were recorded on a U400 or U500 Varian FT-NMR spectrometer. Chemical shifts (δ) are reported in parts per million (ppm) downfield from internal tetramethylsilane or by reference to proton resonances resulting from incomplete deuteration of the NMR solvent. Low- and high-resolution electron impact (EI) and chemical ionization (CI) mass spectra were performed in the Mass Spectrometry Lab of the University of Illinois. Elemental analyses were performed by the Microanalytical Service Laboratory of the University of Illinois. Melting points were determined on a Thomas-Hoover melting point apparatus and are uncorrected. Radiolabeled estradiol ([^{3}H]E_2) ([6,7-^{3}H]estra-1,3,5,(10)-triene-3,17-β-diol), 54 Ci/mmol, was obtained from Amersham Biosciences (Piscataway, NJ). Isopropyl β-D-thiogalactopyranoside, imidazole, β-mercaptoethanol, estradiol, and *trans*-4-hydroxytamoxifen were obtained from Sigma Chemical Co. (St. Louis, MO). The NR box 2 peptide of SRC-1 (SRC-1-NR box 2 residues 683−696, CLTERHKILHRLLQE) was synthesized as described previously.[22]

Relative binding affinity (RBA) analyses were performed according to literature methods.[45,46] Fluorescence experiments used a Perkin-Elmer Life Science Wallac Victor^2 V 1420 multilabel HTS counter with Wallac 1420 workstation software (PerkinElmer, Boston, MA). All data were analyzed using Prism 3.00 (GraphPad Software, San Diego, CA). ER preparations used in these experiments were lamb uterine cytosol, purified full-length human ERα and ERβ (PanVera Inc.), or purified His_6-tagged ERα LBD (304−554).[46] Chemical syntheses of all intermediate compounds are available in the Supporting Information.

The nuclear receptor interaction box 2 peptide (NR-2), corresponding to the NR-2 box sequence of SRC-1, and the octapeptide for fluorophore labeling (see the text) were synthesized by the University of Illinois Biotechnology Center, utilizing FMoc solid-phase strategy on a multiple peptide synthesizer and were purified by C_{18} reversed phase HPLC. The octapeptide was labeled on the N-terminus with rhodamine using the succinimidyl ester. Peptide quality was determined by analytical HPLC and mass spectroscopy (University of Illinois Biotechnology Center).

Chemical Synthesis. General Procedure for Triaminotriazenes. Isobutylamine (1.78 mL, 17.9 mmol) and diisopropylamine (2.35 mL, 17.9 mmol) were dissolved in DMF (10 mL). Cyanuric chloride (1.0 g, 5.4 mmol) was added. The reaction bubbled vigorously and a precipitate formed which dissolved after 30 min of heating. The reaction mixture was refluxed for 16 h. Upon cooling, a precipitate formed which was filtered. The filtrate was extracted with CH_2Cl_2, and the extracts were dried over $NaSO_4$ and concentrated under reduced pressure.

***N,N′,N″*-Triisobutylmelamine (1a).** Triazene **1a** was prepared according to the general procedure for the synthesis of triaminotriazenes. Flash chromatography (75:25 hexane:EtOAc) afforded **1** as a white waxy residue (405 mg, 43%): ^{1}H NMR (500 MHz, $CDCl_3$) δ 1.19 (d, 6H, J = 6.76 Hz, CH_3), 1.81 (bs, 1H, CH), 3.17 (bs, 2H, CH_2), 4.70 (bs, 1 H, NH); ^{13}C NMR (125 MHz, $CDCl_3$) δ 20.2, 28.6, 48.2, 116.5; LRMS (EI, 70 eV) *m*/*z* 294 (M^+); HRMS (EI) calcd for $C_{15}H_{30}N_6$ 294.2532, found 294.2529.

***N,N′,N″*-Tripropylmelamine (1b).** Triazene **1b** was prepared according to the general procedure for the synthesis of triaminotriazenes. Flash chromatography (1:1 EtOAc:hexane) provided the product as a yellow oil (368 mg, 27%): ^{1}H NMR ($CDCl_3$, 400 mHz) δ 0.89 (t, 9H, J = 7.40 Hz, CH_3), 1.51 (sextet, 6H, J = 6.93 Hz, CH_2CH_3), 3.27 (bs, 6H, CH_2NH), 5.19 (bs, 3H, NH); ^{13}C NMR ($CDCl_3$, 125 MHz) δ 11.3, 22.9, 42.3, 165.9; LRMS (EI, 70 eV) *m*/*z* 252.2 (M^+), 237.2 ($M^+ - CH_3$), 223.2 ($M^+ - CH_2CH_3$); HRMS calcd for $C_{12}H_{24}N_6$ 252.2062, found 252.2069.

***N,N′,N″*-Tribenzylmelamine (1c).**[47] Triazene **1c** was prepared according to the general procedure for the synthesis of triaminotriazenes. Recrystallization from EtOH followed by flash chromatography (75:25 hexane:EtOAc) provided the product as an off white solid (491 mg, 23%): mp 90−93 °C; ^{1}H NMR ($CDCl_3$, 400 mHz) δ 4.55 (bs, 2H, CH_2), 5.25 (bd, 1H, NH), 7.18−7.36 (m, 5H, ArH); ^{13}C NMR ($CDCl_3$, 125 MHz) δ 44.6, 127.1, 127.6, 128.5, 139.2, 160.9; LRMS (EI, 70 eV) *m*/*z*

396.2 (M^+), 305.2 ($M^+ - C_7H_7$); HRMS calcd for $C_{24}H_{24}N_6$ 396.2062, found 396.3062.

***N,N′,N″*-Tris(cyclohexylmethyl)melamine (1d).** Triazene **1d** was prepared according to the general procedure for the synthesis of triaminotriazenes. Flash chromatography (75:25 hexane:EtOAc) provided the product as an off-white oil (53 mg, 2.3%): ^{1}H NMR ($CDCl_3$, 400 MHz) δ 0.94 (m, 2H, CH_2), 1.19 (m, 3H, aliphH), 1.50 (m, 1H, CH), 1.71 (m, 5H, aliphH), 3.15 (m, 2H, NHCH_2), 4.92 (bd, 1H, NH); ^{13}C NMR ($CDCl_3$, 125 MHz) δ 25.9, 26.5, 30.9, 38.2, 46.9, 166.0; LRMS (EI, 70 eV) *m/z* 414.4 (M^+), 346.4 ($M^+ - C_6H_{10}$), 318.3 ($M^+ - C_7H_{12}$); HRMS calcd for $C_{24}H_{42}N_6$ 414.3471, found 414.3467.

***N,N′,N″*-Tris(1-naphthylmethyl)melamine (1e).** Triazene **1e** was prepared according to the general procedure for the synthesis of triaminotriazenes. Flash chromatography (1:1 EtOAc:hexane) provided the product as a solid which was recrystallized from EtOH (256 mg, 49%): mp 115−117 °C; ^{1}H NMR ($CDCl_3$, 500 MHz) δ 4.95 (d, 2H, J = 5.62 Hz, CH_2), 5.74 (bs, 1H, NH), 7.50 (m, 3H, ArH), 7.84 (dd, 1H, J = 7.32, 2.20 Hz, ArH), 7.89 (m, 1H, ArH), 7.89 (m, 1H, ArH); ^{13}C NMR ($CDCl_3$, 125 MHz) δ 40.2, 123.3, 124.9, 125.3, 126.1, 126.7, 126.8, 128.7, 131.2, 132.8, 133.8, 160.7.

***N,N′*-Diisobutyl-6-(3-methylbutyl)[1,3,5]triazene-2,4-diamine (3).** Crude monoaminodichlorotriazene **2** (0.47 mL, 2.1 mmol) was dissolved in THF (10 mL). Isobutylamine (0.52 mL, 5.3 mmol) and diisopropylamine (0.7 mL, 5.3 mmol) were added. The reaction mixture was refluxed for 16 h. After cooling, the reaction mixture was poured over water. The residue was extracted with EtOAc, and the extracts were washed with H_2O and brine, dried over $NaSO_4$, and concentrated at reduced pressure. Flash chromatography (9:1 hexane:EtOAc) afforded the product as a light yellow solid (0.34 g, 55%): mp 89−90 °C; ^{1}H NMR ($CDCl_3$, 500 MHz) δ 0.92 (d, 6 H, J = 6.3 Hz, CH(CH_3)$_2$), 0.94 (d, 12 H, J = 6.92 Hz, NHCH$_2$-CH(CH_3)$_2$), 1.59 (m, 3 H, CH), 1.84 (bs, 2 H, CHCH_2CH$_2$), 2.40 (bs, 2 H, CHCH$_2$CH_2), 3.32 (s, 4 H, CH_2NH), 5.01 (bs, 1 H, NH), 5.19 (bs, 1 H, NH); ^{13}C NMR ($CDCl_3$, 125 MHz) δ 20.2, 22.4, 28.3, 28.5, 37.0, 48.1, 133, 166.1; LRMS (EI, 70 eV) *m/z* 294.2 (M^+); HRMS calcd for $C_{16}H_{31}N_5$ 293.2579, found 293.2567.

{Isobutyl[4-isobutylamino-6-(3-methylbutyl)[1,3,5]-triazin-2-yl]amino}acetic Acid (7a). Triazene **6a** (57 mg, 0.15 mmol) was dissolved in 3 mL of methanol at room temperature. Then 0.25 mL of 4 M NaOH was added dropwise. After stirring for 18 h, the reaction was partitioned between EtOAc and brine, and the extracts were dried over $NaSO_4$ and concentrated to a white solid (43.6 mg, 83%). No further purification was necessary: mp 175−181 °C; ^{1}H NMR ($CDCl_3$, 400 MHz) major rotamer δ 0.94 (m, 18H, 6 × CH_3), 1.60 (m, 3H, CH_2CH), 1.92 (m, 2H, 2 × CH), 2.66 (t, 2H, J = 7.32 Hz, ArCH_2), 3.03 (t, 2H, J = 6.34 Hz, NHCH_2CH), 3.56 (d, 2H, J = 7.32 Hz, NCH_2CH), 4.18 (s, 2H, CH_2CO); minor rotamer δ 0.85 (m, 18H, 6 × CH_3), 1.60 (m, 3H, CH_2CH), 1.92 (m, 2H, 2 × CH), 2.57 (t, 2H, J = 7.32 Hz, ArCH_2), 3.21 (t, 2H, J = 6.22 Hz, NHCH_2CH), 3.44 (d, 2H, J = 7.32 Hz, NCH_2CH), 4.33 (s, 2H, CH_2CO); ^{13}C NMR ($CDCl_3$, 125 MHz) both rotamers δ 19.9, 20.0, 20.1, 20.2, 22.0, 22.1, 27.1, 27.38, 27.45, 27.47, 27.95, 28.04, 32.5, 32.6, 34.6, 34.7, 48.0, 48.2, 50.5, 50.7, 56.5, 56.7, 155.1, 155.5, 162.7, 162.9, 168.9, 169.1, 170.7, 171.2; LRMS (EI, 70 eV) *m/z* 351.3 (M^+), 336.3 ($M^+ - CH_3$), 308.3 ($M^+ - C_3H_7$); HRMS calcd for $C_{18}H_{33}N_5O_2$ 351.2634, found 351.2639.

{[4-Isobutylamino-6-(3-methylbutyl)[1,3,5]triazin-2-yl]-isopropylamino}acetic Acid (7b). Triazene **6b** (130 mg, 0.36 mmol) was dissolved in 3 mL of methanol. Then 0.44 mL of 4 M NaOH was added slowly. After stirring for 18 h, the reaction was partitioned between EtOAc and brine, and the extracts were dried over $NaSO_4$ and concentrated to a white residue (59.3 mg, 49%). No further purification was necessary: ^{1}H NMR ($CDCl_3$, 400 MHz) rotameric mixture δ 0.86 (m, 12H, CH_3), 1.20 (m, 6H, (CH_3)$_2$CHN), 1.57 (m, 3H, CH_2CH), 1.85 (m, 1H, CH), 2.53 (m, 2H, CH_2), 3.15 (m, 2H, CH_2CO$_2$H), 4.85−5.20 (m, 1H, NCH), 9.09 (bs, 1H, OH); ^{13}C NMR ($CDCl_3$, 125 MHz) rotameric mixture δ 19.6, 19.7, 20.0, 20.05, 20.06, 20.09, 20.16, 20.17, 22.08, 22.13, 27.33, 27.39, 27.6, 27.64, 27.98, 28.05, 28.14, 28.16, 32.64, 32.8, 33.05, 34.82, 34.87, 35.05, 35.20, 43.85, 43.96, 45.31, 45.37, 47.18, 47.29, 47.47, 47.69, 47.92, 48.06, 48.08, 48.15, 52.18, 52.25, 155.82, 156.35, 156.98, 161.75, 161.9, 162.29, 169.35, 173.75, 173.95; LRMS (EI, 70 eV) *m/z* 336.2 (M^{-1}), 320.0 ($M^+ - OH$), 308.2 ($M^+ - C_2H_5$); HRMS calcd for $C_{17}H_{30}N_5O_2$ 336.2399, found 336.2397.

General Procedure for 2-Thioxo-2,3-1*H*-pyrimidin-4-ones. Thiourea (1 g, 13.0 mmol) was dissolved in 1.6 mL of water at 70 °C. β-Keto ester (3.4 g, 19.7 mmol) was added followed by K_2CO_3 (2.73 g, 19.37 mmol), upon which the solution became cloudy. It was heated to 105 °C, where the precipitate dissolved. The reaction was heated at this temperature open to air for 1 h, boiling off any remaining ethanol and leaving a light yellow solid. Heat was removed and the reaction allowed to cool to room temperature over a period of 2 h. Water (6.6 mL) was added followed by 6 mL of concentrated HCl, causing the reaction to bubble vigorously. The white precipitate was collected and washed with water and 1 M HCl.

General Procedure for Conversion of Thiouracil to Uracil Derivatives. Chloroacetic acid (1.34 g, 0.0142 mol) was dissolved in H_2O (5 mL). Crude **5** (1.4 g, 0.0071mol) was dissolved in H_2O/THF and added to the stirring solution. The reaction mixture was refluxed for 6 h. Concentrated HCl (0.36 mL) was added carefully, and the reaction returned to reflux for 12 h. The reaction mixture was extracted with ether/THF, washed with H_2O, dried over $NaSO_4$, and concentrated at reduced pressure.

General Procedure for Conversion of Uracil Derivatives to Dichloropyrimidines. *n*-Butyluracil **10a** (1 g, 5.9 mmol) was suspended in 9 mL of $POCl_3$ and heated to reflux. After 20 min of heating, the reaction became homogeneous. After 3 h, the reaction was cooled to room temperature and concentrated at reduced pressure. The residue was diluted with 30 mL of ice water. After 1 h, the residue was partitioned between EtOAc and H_2O, and the extracts were dried over $NaSO_4$ and concentrated at reduced pressure.

General Procedure for Substitution of Dichloropydrimidines. Pyrimidine **11a** (152 mg, 0.685 mmol) was dissolved in diisopropylamine (0.90 mL, 6.85 mmol) and isobutylamine (0.68 mL, 6.85 mmol). The reaction was refluxed for 12 h. After cooling it was extracted with CH_2Cl_2, and the extracts were dried over $NaSO_4$ and concentrated under vacuum.

***N*^{2},*N*^{4}-Diisobutyl-6-(3-methylbutyl)pyrimidine-2,4-diamine (12a).** Pyrimidine **12a** was synthesized according to the general procedure for the substitution of dichloropydrimidines. Flash chromatography afforded the product (175 mg, 60%) as a yellow solid: ^{1}H NMR ($CDCl_3$, 500 MHz) δ 0.89 (d, 6 H, J = 6.68 Hz, CH_3), 0.93 (d, 6 H, J = 6.58 Hz, NHCH$_2$-CH(CH_3)$_2$), 0.93 (d, 6 H, J = 6.43 Hz, NHCH$_2$CH(CH_3)$_2$), 1.49 (q, 2 H, J = 7.66 Hz, CHCH_2CH$_2$), 1.58 (nonet, 1 H, J = 6.49, CH), 1.83 (nonet, 2 H, J = 6.75 Hz, CHCH$_2$NH), 2.38 (t, 2 H, J = 8.06 Hz, CHCH$_2$CH_2), 3.05 (bs, 1 H, NH), 3.15 (t, 2 H, J = 6.23 Hz, CHCH_2NH), 4.78 (bs, 1 H, NH), 5.50 (s, 1 H, C=CH); ^{13}C NMR ($CDCl_3$, 125 MHz) δ 20.2/20.3, 22.4, 27.9, 28.4/28.5, 35.5, 37.8, 48.9, 91.0, 162.1, 163.8; LRMS (EI, 70 eV) *m/z* 293.3 (M^+) 249.2 ($M^+ - C_3H_8$); HRMS calcd for $C_{17}H_{33}N_4$ 293.2705, found 293.2704.

6-Butyl-2,4-(propylamino)pyrimidine (12b). Pyrimidine **12b** was synthesized according to the general procedure for the substitution of dichloropydrimidines. Flash chromatography (1:1 EtOAc:hexane) provided the product as an oil (12 mg, 9.4%) along with both monoaminated products accounting for the remainder of the mass balance: ^{1}H NMR ($CDCl_3$, 400 MHz) δ 0.91 (t, 3H, J = 7.32 Hz, CH_3), 0.95 (t, 3H, J = 6.84 Hz, CH_3), 0.96 (t, 3H, J = 6.84 Hz, CH_3), 1.36 (sextet, 2H, J = 7.42 Hz, CH_2CH$_3$), 1.59 (m, 6H, 3 × CH_2), 2.39 (dd, 2H, J = 8.06 Hz, 7.57, CH_2Ar), 3.20 (q, 2H, J = 6.43 Hz, CH_2NH), 4.63 (bs, 1H, NH), 4.86 (bs, 1H, NH), 5.53 (s, 1H, CH); ^{13}C NMR ($CDCl_3$, 125 MHz) δ 11.46 (2), 11.51, 13.9, 22.5, 22.7, 23.0, 109.7, 162.2, 163.8 (2); LRMS (EI, 70 eV) *m/z* 250.2 (M^+), 235.2 ($M^+ - CH_3$), 221.2 ($M^+ - C_2H_3$); HRMS calcd for $C_{14}H_{26}N_4$ 250.2157, found 250.2153.

6-(2-Phenylethyl)-2,4-(benzylamino)pyrimidine (12c). Pyrimidine **12c** was synthesized according to the general procedure for the substitution of dichloropydrimidines. Flash chromatography (1:1 EtOAc:hexane) provided the product (16 mg, 51%) as a yellow oil: ^{1}H NMR ($CDCl_3$, 400 MHz) δ 2.70 (AB_q, 2H, $\nu_a = 2.73$, $\nu_b = 2.67$, $J_{ab} = 5.60$ Hz, C*H*$_2$), 2.83 (AB_q, 2H, $\nu_a = 2.98$, $\nu_b = 2.71$, $J_{ab} = 7.15$ Hz, C*H*$_2$), 4.48 (bd, 2H, $J = 4.39$ Hz, CH_2NH), 4.58 (d, 2H, $J = 5.86$ Hz, C*H*$_2$NH), 5.55 (s, 1H, C*H*), 7.25 (m, 15H, Ar*H*); ^{13}C NMR ($CDCl_3$, 125 MHz) δ 34.1, 44.9, 45.1, 93.7, 126.2, 127.0, 127.5, 127.55, 127.59, 128.4, 128.7, 138.0, 139.1, 140.6, 163.3; LRMS (EI, 70 eV) 394.2 (M^+), 317.2 ($M^+ - C_6H_5$), 303.2 ($M^+ - C_7H_7$); HRMS calcd for $C_{26}H_{26}N_4$ 394.2157, found 394.2154.

2,4,6-Tris(3-methylbutyl)[1,3,5]trithiane (13). 1,3,5-Trithiane (250 mg, 1.81 mmol) was suspended in THF (10 mL) and cooled to −35 °C. *n*-Butyllithium (1.25 mL, 1.99 mmol) was added dropwise. The reaction was allowed to warm to room temperature and stir for 45 min. The reaction was then cooled to −20 °C and 3-methylbutyl bromide (0.32 mL, 2.71 mmol) was added dropwise. The reaction was warmed to room temperature and stirred for 1.5 h. The procedure was repeated two additional times, allowing the reaction to stir at room temperature for 12 h after the final addition of the bromide. The reaction was quenched with H_2O (5 mL) and extracted with chloroform, and the extracts were dried over $NaSO_4$ and concentrated at reduced pressure. Flash chromatography (98:2 hexane:EtOAc) afforded a light yellow solid which was recrystallized from 2-propanol to give white crystals (340 mg, 54% yield): mp 60−62 °C; ^{1}H NMR ($CDCl_3$, 500 MHz) δ 0.89 (d, 6H, $J = 6.51$ Hz, CH_3), 1.46 (m, 2H, $(CH_3)_2CHCH_2$), 1.56 (nonet, 1H, $J = 6.54$ Hz, $(CH_3)_2CH$), 1.87 (m, 2H, CH_2CHS), 4.10 (t, 1H, $J = 6.45$ Hz, CHS); ^{13}C NMR ($CDCl_3$, 125 MHz) δ 22.3, 27.9, 33.4, 35.3, 54.1; LRMS (EI, 70 eV) *m*/*z* 348.1 (M^+); HRMS calcd for $C_{16}H_{36}S_3$ 348.1979, found 348.1984.

1,3,5-Trimethylcyclohexane-1,3,5-tricarboxylic Acid Tris(isobutyl amide) (14). Kemp's triacid (200 mg, 0.77 mmol), isobutylamine (0.39 mL, 3.87 mmol), and HOBt (522 mg, 3.87 mmol) were added to 10 mL of DMF and cooled to 0 °C. Triethylamine (1.08 mL) was added, and the reaction stirred for 5 min. EDC (742 mg, 3.87 mmol) was added and the reaction allowed to warm to room temperature. The reaction was refluxed for 12 h after which the DMF was distilled off under house vacuum. The residue was taken up in CH_2Cl_2 and washed with brine and $NaHCO_3$, and the extracts were dried over $NaSO_4$ and concentrated under vacuum. Flash chromatography (75:25 hexane:EtOAc) provided the product (289 mg, 88%) as a yellow oil: ^{1}H NMR ($CDCl_3$, 400 MHz) δ 0.88 (d, 18H, $J = 6.59$ Hz, $(CH_3)_2CH$), 1.05 (d, 3H, $J = 15.63$ Hz, CH(ring)), 1.22 (s, 9H, CH_3), 1.75 (septuplet, 3H, CH), 2.90 (m, 9H, CH(ring) and C*H*$_2$NH), 7.51 (bt, 3H, $J = 5.37$ Hz, NH); ^{13}C NMR ($CDCl_3$, 125 MHz) δ 20.1, 25.9, 27 LRMS (EI, 70 eV) *m*/*z* 252.2 ($M^{+)}$.1, 28.4, 31.9, 40.2, 42.1, 43.6, 44.8, 46.4, 47.0, 173.4, 176.8; LRMS (EI, 70 eV) *m*/*z* 423.1 (M^+), 351.3 ($M^+ - C_4H_{10}N$); HRMS calcd for $C_{24}H_{45}N_3O$ 423.3461, found 423.3458.

2,7-Bis[2-(4-methylpentanoylamino)ethyl]naphthalene (18a). Naphthalene **17** (30 mg, 0.14 mmol) was combined with 3-methylbutyl acid choride (0.043 mL. 0.31 mmol) and triethylamine (0.043 mL, 0.31 mmol) in 2 mL of CH_2Cl_2. The reaction was refluxed for 4 h. After cooling, the reaction was partitioned between EtOAc and water/brine, and the extracts were dried over $NaSO_4$ and concentrated under vacuum. The crude solid was recrystallized from hexane/CH_2Cl_2 (25 mg, 45%). Mp 179−180 °C. Material for binding assay was further purified by reversed phase HPLC (hexane:ethanol 85:15): ^{1}H NMR ($CDCl_3$, 400 MHz) δ 0.84 (d, 12H, $J = 6.10$ Hz, CH_3), 1.49 (m, 6H, $CHCH_2$), 2.10 (t, 4H, $J = 7.69$ Hz, CH_2CO), 2.96 (t, 4H, $J = 6.84$ Hz, CH_2Ar), 3.59 (q, 4H, $J = 6.59$ Hz, C*H*$_2$-NH), 5.56 (bs, 2H, NH), 7.30 (d, 2H, $J = 8.06$ Hz, $H_{3,6}$), 7.56 (s, 2H, $H_{1,8}$), 7.76 (d, 2H, $H_{4,5}$); ^{13}C NMR ($CDCl_3$, 100 MHz) δ 22.3, 27.7, 34.6, 35.9, 40.4, 126.7, 126.8, 128.0, 131.0, 133.6, 136.8, 173.3; LRMS (EI. 70 eV) *m*/*z* 410.4 (M^+); HRMS calcd for $C_{26}H_{38}N_2O_2$ 410.2933, found 410.2936.

2,7-Bis[2-((3-methylpentanoyl)amino)ethyl]naphthalene (18b). Naphthalene **17** (30 mg, 0.14 mmol) was combined with 2-methylbutyl acid choride (0.042 mL, 0.31 mmol) and triethylamine (0.043 mL, 0.31 mmol) in 2 mL of CH_2Cl_2. The reaction was refluxed for 6 h. After cooling, the reaction was partitioned between EtOAc and water/brine, and the extracts were dried over $NaSO_4$ and concentrated under vacuum. Flash chromatography (95:5 CH_2Cl_2:MeOH) provided the product (41.8 mg, 73%) as a white powder which was recrystallized from hexane:EtOH. Mp 179−181 °C. Material for binding assay was further purified by reversed phase HPLC (hexane: ethanol 85:15): ^{1}H NMR ($CDCl_3$, 400 MHz) δ 0.87 (m, 12H, CH_3), 1.15 (m, 2H, CH_3CH_2), 1.33 (m, 2H, CH_3CH_2), 2.05 (m, 6H, $CHCH_2CO$), 2.97 (t, 4H, $J = 6.96$ Hz $ArCH_2$), 3.61 (q, 4H, $J = 6.47$ Hz, C*H*$_2$NH), 5.46 (bs, 2H, NH), 7.31 (dd, 2H, $J = 8.30$ Hz, 1.46, $H_{3,6}$), 7.57 (bs, 2H, $H_{1,8}$), 7.77 (d, 2H, $J = 8.30$ Hz, $H_{4,5}$); ^{13}C NMR ($CDCl_3$, 125 MHz) δ 11.3, 19.1, 29.3, 32.3, 35.9, 40.4, 44.2, 126.7, 126.8, 128.1, 130.1, 133.7, 136.8, 172.7; LRMS (EI, 70 eV) *m*/*z* 410.4 (M^+), 367.4 ($M^+ - C_3H_7$), 341.4 ($M^+ - C_5H_9$); HRMS calcd for $C_{26}H_{38}N_2O_2$ 410.2933, found 410.2927.

Fluorescence Anisotropy Assays. Purified ERα ligand binding domain and tetramethylrhodamine-labeled NR box peptide (*ILRKLLQE) were used for the fluorescence anisotropy assays. The His_6-tagged ERα-LBD (304−554) was expressed from a pET-15b vector in BL21(DE3)pLysS *Escherichia coli* and purified as described previously.[46] A stock solution (9 μL) of ERα-LBD (444 nM), estradiol (22 μM), and ovalbumin (0.3 mg/mL) in Tris-glycerol buffer (50 mM Tris, 10% glycerol, pH 8.0) was placed in separate wells of a black 96-well Molecular Devices HE high efficiency microplate (Molecular Devices, Inc., Sunnyvale, CA) and incubated at room temperature for 1 h in the dark. In a second 96-well Nunc polypropylene plate (Nalge Nunc International, Rochester, NY), a solution of the coactivator binding inhibitor (556 μM) was serially diluted in a 1:10 fashion into ovalbumin (0.3 mg/mL) in Tris-glycerol (pH 8.0) buffer. Each concentration of CBI (9 μL) or vehicle (buffer) was transferred into the 96-well Molecular Devices plate, and the background fluorescence signal was measured with a 544/15 nm excitation and 590/10 nm emission filter pair to correct for any autofluorescence artifacts from ligand or CBI in our experiments. A 2 μL solution of the TMR−peptide (200 nM) and ovalbumin (0.3 mg/mL) in Tris-glycerol (pH 8.0) buffer was added to each well of the 96-well Molecular Devices plate. The final concentrations of the reagents were as follows: ERα (200 nM), estradiol (10 μM), CBI (0−250 μM), TMR−peptide (20 nM). The plate was incubated at room temperature for 1.5 h in the dark and the fluorescence anisotropy measured with a 544/15 nm excitation and 590/10 nm emission filter pair. Correction was made for any change in fluorescence intensity of TMR−peptide between its bound vs free state, according to the method recommended by PanVera (PanVera Fluorescence Polarization Applications Guide; PanVera Corp., Madison, WI).

Molecular Modeling. The X-ray crystal structure of the estrogen receptor bound to diethylstilbestrol and the GRIP1 peptide (ERD in the protein data bank) was used for modeling purposes. The starting conformations for all ligands were generated using the MMFF94 force field in SYBYL, by minimizing to a gradient of 0.05 kcal/mol. The minimized CBI was then prepositioned in the coactivator binding groove by overlaying it onto the GRIP1 peptide using a least-squares multifitting of select atoms with the ligand. Once positioned, GRIP1 was deleted. Rotatable bonds in the CBI were chosen and the CBI docked into the receptor using the FlexiDock routine within the BioPolymer module of SYBYL beginning on a random seed, allowing 25 000 interations. The lowest energy solution was then extracted from the receptor and the docking process repeated a second time, this time allowing both the ligand and side chains of the receptor within 5 Å of the ligand to have rotatable bonds. The lowest energy solution was then put through a three-step minimization protocol as previously described.[48]

Acknowledgment. We are grateful for support of this research through a grant from the U.S. Army Breast Cancer Research Program (DAMD17-00-1-0293). NMR spectra were obtained in the Varian Oxford Instrument Center for Excellence in NMR Laboratory. Funding for the instrumentation was provided in part by the W.M. Keck Foundation, the National Institutes of Health (PHS 1 S10 RR104444-01), and the National Science Foundation (NSF CHE 96-10502). Mass spectra were obtained on instruments supported by grants form the National Institute of General Medical Sciences (GM 27029), the National Instituted of Health (RR 01575), and the National Science Foundation (PCM 8121494).

Supporting Information Available: A description of the synthesis of compounds **2**, **4**, **6a**−**b**, **9a**−**c**, **10a**−**c**, **11a**−**c**, **15**, **16**, and **17**. This information is available free of charge via the Internet at http://pubs.acs.org.

References

(1) McKenna, N. J.; O'Malley, B. W. Minireview: Nuclear receptor coactivators—an update. *Endocrinology* **2002**, *143*, 2461−2465.
(2) McKenna, N. J.; O'Malley, B. W. Combinatorial control of gene expression by nuclear receptors and coregulators. *Cell* **2002**, *108*, 465−474.
(3) Shiau, A. K.; Barstad, D.; Loria, P. M.; Cheng, L.; Kushner, P. J.; et al. The structural basis of estrogen receptor/coactivator recognition and the antagonism of this interaction by tamoxifen. *Cell* **1998**, *95*, 927−937.
(4) Shiau, A. K.; Barstad, D.; Radek, J. T.; Meyers, M. J.; Nettles, K. W.; et al. Structural characterization of a subtype-selective ligand reveals a novel mode of estrogen receptor antagonism. *Nat. Struct. Biol.* **2002**, *9*, 359−364.
(5) Darimont, B. D.; Wagner, R. L.; Apriletti, J. W.; Stallcup, M. R.; Kushner, P. J.; et al. Structure and specificity of nuclear receptor−coactivator interactions. *Genes Dev.* **1998**, *12*, 3343−3356.
(6) Gampe, R. T.; Montana, V. G.; Lambert, M. H.; Miller, A. B.; Bledsoe, R. K.; et al. Asymmetry in the PPARgamma/RXRalpha crystal structure reveals the molecular basis of heterodimerization among nuclear receptors. *Mol. Cell* **2000**, *5*, 545−555.
(7) Egea, P. F.; Mitschler, A.; Moras, D. Molecular recognition of agonist ligands by RXRs. *Mol. Endo.* **2002**, *16*, 987−997.
(8) Warnmark, A.; Treuter, E.; Gustafsson, J.; Hubbard, R. E.; Brzozowski, A. M.; et al. Interaction of transcriptional intermediary factor 2 nuclear receptor box peptides with the coactivator binding site of estrogen receptor alpha. *J. Biol. Chem.* **2002**, *277*, 21862−21868.
(9) Xu, H. E.; Stanley, T. B.; Montana, V. G.; Lambert, M. H.; Shearer, B. G.; et al. Structural basis for antagonist-mediated recruitment of nuclear co-repressors by PPAR alpha. *Nature* **2002**, *415*, 813−817.
(10) Mi, L. Z.; Devarakonda, S.; Harp, J. M.; Han, Q.; Pellicciari, R.; et al. Structural Basis for Bile Acid Binding and Activation of the Nuclear Receptor FXR. *Mol. Cell* **2003**, *11*, 1093−1100.
(11) Downes, M.; Verdecia, M. A.; Roecker, A. J.; Hughes, R.; Hogenesch, J. B.; et al. A Chemical, Genetic, and Structural Analysis of the Nuclear Bile Acid Receptor FXR. *Mol. Cell* **2003**, *11*, 1079−1092.
(12) Brzozowski, A. M.; Pike, A. C.; Dauter, Z.; Hubbard, R. E.; Bonn, T.; et al. Molecular basis of agonism and antagonism in the oestrogen receptor. *Nature* **1997**, *389*, 753−758.
(13) Pike, A. C.; Brzozowski, A. M.; Hubbard, R. E.; Bonn, T.; Thorsell, A. G.; et al. Structure of the ligand-binding domain of oestrogen receptor beta in the presence of a partial agonist and a full antagonist. *EMBO J.* **1999**, *18*, 4608−4618.
(14) Pike, A. C.; Brzozowski, A. M.; Walton, J.; Hubbard, R. E.; Thorsell, A. G.; et al. Structural insights into the mode of action of a pure antiestrogen. *Structure (Camb)* **2001**, *9*, 145−153.
(15) Shang, Y.; Brown, M. Molecular determinants for the tissue specificity of SERMs. *Science* **2002**, *295*, 2465−2468.
(16) Schiff, R.; Massarweh, S.; Shou, J.; Osborne, C. K. Breast cancer endocrine resistance: How growth factor signaling and estrogen receptor coregulators modulate response. *Clin. Cancer Res.* **2003**, *9*, 447S-454S.
(17) Osborne, C. K.; Bardou, V.; Hopp, T. A.; Chamness, G. C.; Hilsenbeck, S. G.; et al. Role of the estrogen receptor coactivator AIB1 (SRC-3) and HER-2/neu in tamoxifen resistance in breast cancer. *J. Natl. Cancer Inst.* **2003**, *95*, 353−361.
(18) Norris, J. D.; Paige, L. A.; Christensen, D. J.; Chang, C. Y.; Huacani, M. R.; et al. Peptide antagonists of the human estrogen receptor. *Science* **1999**, *285*, 744−746.
(19) Connor, C. E.; Norris, J. D.; Broadwater, G.; Willson, T. M.; Gottardis, M. M.; et al. Circumventing tamoxifen resistance in breast cancers using antiestrogens that induce unique conformational changes in the estrogen receptor. *Cancer Res* **2001**, *61*, 2917−2922.
(20) Pope, A. J.; Haupt, U. M.; Moore, K. J. Homogeneous fluorescence readouts for miniaturized high-throughput screening: Theory and practice. *Drug Discov. Today* **1999**, *4*, 350−362.
(21) Jameson, D. M.; Seifried, S. E. Quantification of protein−protein interactions using fluorescence polarization. *Methods* **1999**, *19*, 222−233.
(22) Gee, A. C.; Carlson, K. E.; Martini, P. G. V.; Katzenellenbogen, B. S.; Katzenellenbogen, J. A. Coactivator peptides have a differential stabilizing effect on the binding of estrogens and antiestrogens with the estrogen receptor. *Mol. Endocrinol.* **1999**, *13*, 1912−1923.
(23) Tamrazi, A.; Carlson, K. E.; Daniels, J. R.; Hurth, K. M.; Katzenellenbogen, J. A. Estrogen receptor dimerization: Ligand binding regulates dimer affinity and dimer dissociation rate. *Mol. Endocrinol.* **2002**, *16*, 2706−2719.
(24) Paige, L. A.; Christensen, D. J.; Gron, H.; Norris, J. D.; Gottlin, E. B.; et al. Estrogen receptor (ER) modulators each induce distinct conformational changes in ER alpha and ER beta. *Proc. Natl. Acad. Sci. U.S.A.* **1999**, *96*, 3999−4004.
(25) Chang, C.; Norris, J. D.; Gron, H.; Paige, L. A.; Hamilton, P. T.; et al. Dissection of the LXXLL nuclear receptor-coactivator interaction motif using combinatorial peptide libraries: Discovery of peptide antagonists of estrogen receptors alpha and beta. *Mol. Cell Biol.* **1999**, *19*, 8226−8239.
(26) Hall, J. M.; Chang, C. Y.; McDonnell, D. P. Development of peptide antagonists that target estrogen receptor beta-coactivator interactions. *Mol Endocrinol* **2000**, *14*, 2010−2023.
(27) Huang, H.-J.; Norris, J. D.; McDonnell, D. P. Identification of a negative regulatory surface within estrogen receptor alpha provides evidence in support of a role for corepressors in regulating cellular responses to agonists and antagonists. *Mol. Endocrinol.* **2002**, *16*, 1778−1792.
(28) McInerney, E. M.; Rose, D. W.; Flynn, S. E.; Westin, S.; Mullen, T. M.; et al. Determinants of coactivator LXXLL motif specificity in nuclear receptor transcriptional activation. *Genes Dev.* **1998**, *12*, 3357−3368.
(29) Geistlinger, T. R.; Guy, R. K. An inhibitor of the interaction of thyroid hormone receptor beta and glucocorticoid interacting protein 1. *J. Am. Chem. Soc.* **2001**, *123*, 1525−1526.
(30) Geistlinger, T. R.; Guy, R. K. Novel selective inhibitors of the interaction of individual nuclear hormone receptors with a mutually shared steroid receptor coactivator 2. *J. Am. Chem. Soc.* **2003**, *125*, 6852−6853.
(31) Leduc, A. M.; Trent, J. O.; Wittliff, J. L.; Bramlett, K. S.; Briggs, S. L.; et al. Helix-stabilized cyclic peptides as selective inhibitors of steroid receptor−coactivator interactions. *Proc. Natl. Acad. Sci. U.S.A.* **2003**, *100*, 11273−11278.
(32) Toogood, P. T. Inhibition of protein−protein association by small molecules: Approaches and progress. *J. Med. Chem.* **2002**, *45*, 1543−1558.
(33) Peczuh, M. W.; Hamilton, A. D. Peptide and protein recognition by designed molecules. *Chem. Rev.* **2000**, *100*, 2479−2494.
(34) Ernst, J. T.; Kutzki, O.; Debnath, A. K.; Jiang, S.; Lu, H.; et al. Design of a protein surface antagonist based on alpha-helix mimicry: Inhibition of gp41 assembly and viral fusion. *Angew. Chem. Int. Ed. Engl.* **2002**, *41*, 278−281.
(35) Kutzki, O.; Park, H. S.; Ernst, J. T.; Orner, B. P.; Yin, H.; et al. Development of a potent Bcl-x(L) antagonist based on alpha-helix mimicry. *J. Am. Chem. Soc.* **2002**, *124*, 11838−11839.
(36) Orner, B. P.; Ernst, J. T.; Hamilton, A. D. Toward proteomimetics: Terphenyl derivatives as structural and functional mimics of extended regions of an alpha-helix. *J. Am. Chem. Soc.* **2001**, *123*, 5382−5383.
(37) Ernst, J. T.; Becerril, J.; Park, H. S.; Yin, H.; Hamilton, A. D. Design and application of an alpha-helix-mimetic scaffold based on an oligoamide-foldamer strategy: Antagonism of the Bak BH3/Bcl-xL complex. *Angew. Chem. Int. Ed. Engl.* **2003**, *42*, 535−539.
(38) Wang, J. L.; Liu, D.; Zhang, Z. J.; Shan, S.; Han, X.; et al. Structure-based discovery of an organic compound that binds Bcl-2 protein and induces apoptosis of tumor cells. *Proc. Natl. Acad. Sci. U.S.A.* **2000**, *97*, 7124−7129.
(39) Liu, D.; Huang, Z. Synthetic peptides and nonpeptidic molecules as probes of structure and function of Bcl-2 family proteins and modulators of apoptosis. *Apoptosis* **2001**, *6*, 453−462.
(40) Huang, Z. The chemical biology of apoptosis. Exploring protein−protein interactions and the life and death of cells with small molecules. *Chem. Biol.* **2002**, *9*, 1059−1072.

(41) Huang, Z. Structural chemistry and therapeutic intervention of protein−protein interactions in immune response, human immunodeficiency virus entry, and apoptosis. *Pharmacol. Ther.* **2000**, *86*, 201−215.
(42) Asada, S.; Choi, Y.; Uesugi, M. A Gene-Expression Inhibitor that Targets an alpha-Helix-Mediated Protein Interaction. *J. Am. Chem. Soc.* **2003**, *125*, 4992−4993.
(43) Pangborn, A. B.; Giardello, M. A.; Grubbs, R. H.; Rosen, R. K.; Timmers, F. J. Safe and convenient procedure for solvent purification. *Organometallics* **1996**, *15*, 1518−1520.
(44) Suffert, J. Simple direct titration of organolithium reagents using N-pivaloyl-o-toluidine and/or N-pivalolyl-o-benzylaniline. *J. Org. Chem.* **1989**, *54*, 509−510.
(45) Katzenellenbogen, J. A.; Johnson, H. J., Jr.; Myers, H. N. Photoaffinity labels for estrogen binding proteins of rat uterus. *Biochemistry* **1973**, *12*, 4085−4092.
(46) Carlson, K. E.; Choi, I.; Gee, A.; Katzenellenbogen, B. S.; Katzenellenbogen, J. A. Altered ligand binding properties and enhanced stability of a constitutively active estrogen receptor: Evidence that an open pocket conformation is required for ligand interaction. *Biochemistry* **1997**, *36*, 14897−14905.
(47) Shigehiro, O.; Tsumomu, S. N,N′,N″-Tribenzylmelamine (Patent written in Japanese). *Jpn. Tokkyo Koho* **1972**, Patent No. JP47021109; Kind B4; Date 19720614; Application No. JP1969-45379; Application Date 19690611.
(48) Stauffer, S. R.; Coletta, C. J.; Tedesco, R.; Sun, J.; Katzenellenbogen, B. S.; et al. Pyrazole Ligands: Structure−Affinity/Activity Relationships of Estrogen Receptor-a Selective Agonists. *J. Med. Chem.* **2000**, *43*, 4934−4947.

JM030404C